LETTERS

Ephrin-B2 controls VEGF-induced angiogenesis and lymphangiogenesis

Yingdi Wang[1]*, Masanori Nakayama[2]*, Mara E. Pitulescu[2]*, Tim S. Schmidt[1]*, Magdalena L. Bochenek[2,3], Akira Sakakibara[1], Susanne Adams[1,2], Alice Davy[4], Urban Deutsch[5], Urs Lüthi[6], Alcide Barberis[6], Laura E. Benjamin[7], Taija Mäkinen[8], Catherine D. Nobes[3] & Ralf H. Adams[1,2]

In development, tissue regeneration or certain diseases, angiogenic growth leads to the expansion of blood vessels and the lymphatic vasculature. This involves endothelial cell proliferation as well as angiogenic sprouting, in which a subset of cells, termed tip cells, acquires motile, invasive behaviour and extends filopodial protrusions[1–3]. Although it is already appreciated that angiogenesis is triggered by tissue-derived signals, such as vascular endothelial growth factor (VEGF) family growth factors, the resulting signalling processes in endothelial cells are only partly understood. Here we show with genetic experiments in mouse and zebrafish that ephrin-B2, a transmembrane ligand for Eph receptor tyrosine kinases, promotes sprouting behaviour and motility in the angiogenic endothelium. We link this pro-angiogenic function to a crucial role of ephrin-B2 in the VEGF signalling pathway, which we have studied in detail for VEGFR3, the receptor for VEGF-C. In the absence of ephrin-B2, the internalization of VEGFR3 in cultured cells and mutant mice is defective, which compromises downstream signal transduction by the small GTPase Rac1, Akt and the mitogen-activated protein kinase Erk. Our results show that full VEGFR3 signalling is coupled to receptor internalization. Ephrin-B2 is a key regulator of this process and thereby controls angiogenic and lymphangiogenic growth.

Eph receptor tyrosine kinases and their plasma-membrane-anchored ephrin interaction partners control cell migration and cytoskeletal organization in many different cell types and tissues. Like other ephrins, ephrin-B2 (encoded by the gene *Efnb2*) can activate several Eph receptors (termed 'forward' signalling), but also has receptor-like ('reverse') signalling activity. The latter involves the docking of signalling molecules to tyrosine phosphorylation sites and a PDZ binding motif in the ephrin-B2 cytoplasmic domain[4–7]. In the vasculature, ephrin-B2 is a marker of arterial endothelial cells[1,8–10], whereas one of the cognate receptors, EphB4, is predominantly expressed in the venous endothelium. Targeted inactivation of *Efnb2* or *Ephb4* in mice impaired angiogenesis and caused embryonic lethality, suggesting reciprocal roles of these two genes[11–13]. Although its precise cellular function in vascular growth has remained unclear, ephrin-B2 is upregulated during physiological and pathological angiogenesis in the adult[14,15].

We have reinvestigated ephrin-B2 expression with *Efnb2–GFP* reporter mice, in which a complementary DNA (cDNA) encoding a fusion between histone H2B and enhanced green fluorescent protein (GFP) has been inserted into the endogenous *Efnb2* locus[16]. The nuclear GFP signal in these mice labelled arterial endothelial cells as well as angiogenic dermal and retinal capillaries, tip cells and stalk cells at the base of sprouts (Fig. 1a, b and Supplementary Fig. 2). Although EphB4 protein levels are highest in veins, retinal capillaries and endothelial sprouts also showed specific staining (Fig. 1a and Supplementary Fig. 2), which is consistent with previous reports[17] and indicates that ephrin-B2 and EphB4 can physically interact in growing blood vessels.

For functional studies in the vasculature, we used inducible loss-of-function genetics (see Methods and Supplementary Fig. 3) to target the *Efnb2* gene selectively in endothelial cells. Significant downregulation of ephrin-B2 was confirmed by immunofluorescence in $Efnb2^{i\Delta EC}$ mutants at embryonic day (E)15.5, just 4 days after the initiation of gene inactivation (Supplementary Fig. 3d). Mutant embryos displayed oedema and haemorrhaging in the skin between E15.5 and E18.5, and significantly reduced angiogenesis (Fig. 1c, d, f and data not shown). Ephrin-B2 is also required for the growth of the retinal vasculature. Induction of gene inactivation during early postnatal development reduced the size and complexity of the endothelial network, tip cell number, sprout length and endothelial cell proliferation (Fig. 1e, g, h and Supplementary Fig. 4). Downregulating the expression of the *efnb2a* gene by morpholino injection into zebrafish embryos compromised filopodial tension from tip cells in growing intersegmental vessels (Supplementary Fig. 5a, b and Supplementary Movies 1 and 2). Fine cellular protrusions and connections were also largely absent in cultured *Efnb2* knockout endothelial cells, which showed reduced ability to form networks in culture (Supplementary Fig. 5c).

To complement the loss-of-function approaches described above, we have used the tetracycline-regulated system[18,19] to overexpress a cyan fluorescent protein-tagged version of ephrin-B2 (CFP–ephrin-B2) in the endothelium in a temporally controlled fashion. Induction of overexpression during early development caused severe vascular defects at E9.5/E10.5 and was incompatible with survival beyond mid-gestation. Delaying the onset of transgene expression extended survival and led to vascular defects later in embryogenesis (Fig. 2a). Characterization of these $Efnb2^{iGOF}$ mutants confirmed the overexpression of ephrin-B2 in arteries, veins, capillaries and lymphatic vessels, the appearance of an additional protein band corresponding to CFP–ephrin-B2 and higher levels of phospho-EphB4 in immunoprecipitates from transgenic tissues (Fig. 2b and Supplementary Fig. 6). Staining with anti-GFP antibodies (recognizing CFP) revealed that the chimaeric protein was concentrated on endothelial protrusions emerging from dermal and retinal blood vessels as well as tip cells and filopodia (Fig. 2c and data not shown). Whole-mount analysis of the $Efnb2^{iGOF}$ dermal vasculature showed a severely compromised

[1]Vascular Development Laboratory, Cancer Research UK London Research Institute, London WC2A 3PX, UK. [2]Department of Tissue Morphogenesis, Max-Planck-Institute for Molecular Biomedicine, and Faculty of Medicine, University of Münster, D-48149 Münster, Germany. [3]Departments of Physiology & Pharmacology and Biochemistry, School of Medical Sciences, University of Bristol, Bristol BS6 6BS, UK. [4]Centre de Biologie du Développement, Université de Toulouse, CNRS, CBD UMR 5547, F-31062 Toulouse cedex 9, France. [5]Theodor Kocher Institute, University of Berne, CH-3012 Bern, Switzerland. [6]Oncalis AG, Schlieren, Switzerland. [7]Beth Israel Deaconess Medical Center, Boston, Massachusetts 02215-5501, USA. [8]Cancer Research UK London Research Institute, Lymphatic Development Laboratory, London WC2A 3PX, UK.
*These authors contributed equally to this work.

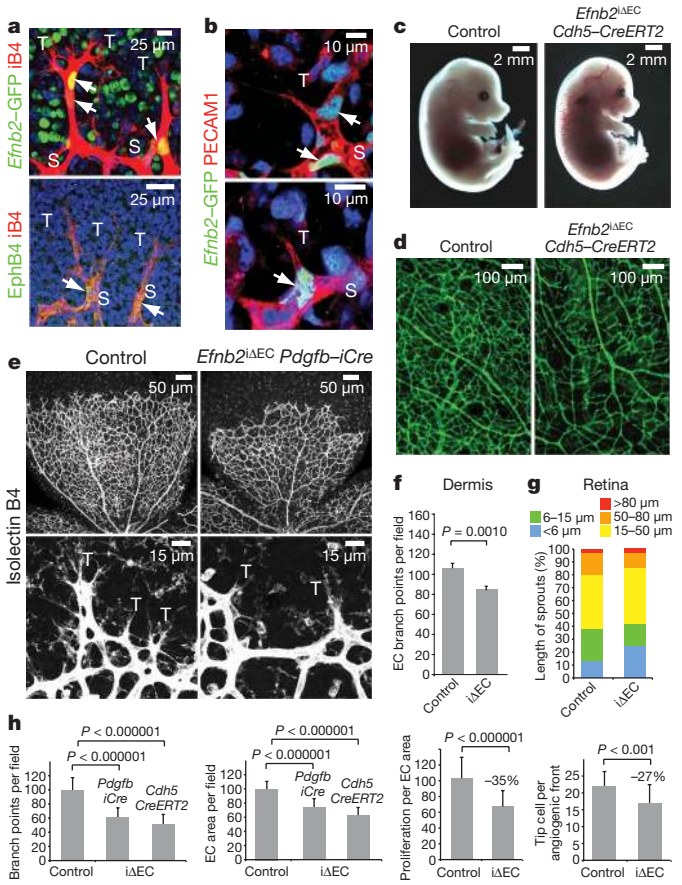

Figure 1 | Ephrin-B2 regulates angiogenesis. **a**, Whole-mount GFP (green) and isolectin B4 (iB4, red) staining of the P5 *Efnb2–GFP* retinal vasculature. Sprout tip (T), stalk (S) and non-vascular cells are positive (arrows). EphB4 immunofluorescence labels stalk cells and is faint in the tip. Nuclei (blue), TO-PRO-3. **b**, *Efnb2–GFP* expression in tip and stalk endothelial cells of the E14.5 dermal vasculature (arrows). Nuclei (blue), 4′,6-diamidino-2-phenylindole (DAPI). **c**, Freshly dissected E15.5 control and mutant embryos. **d**, Anti-PECAM1 staining of the E15.5 dermal vasculature. **e**, Defects in the P6 *Efnb2*$^{i\Delta EC}$ retinal vasculature. Branching and tip cell (T) number are reduced. **f**, Quantification of endothelial cell branch points in E15.5 dermal vessels. **g**, **h**, Endothelial cell branch points and endothelial cell area in control and mutant (iΔEC) retinas with two different Cre lines. Proliferation, tip cell number and sprout length were analysed for *Pdgfb–iCre* only. *P* values (**f**, **h**) were calculated using two-tailed Student's *t*-test ($n \geq 3$). Error bars, s.e.m.

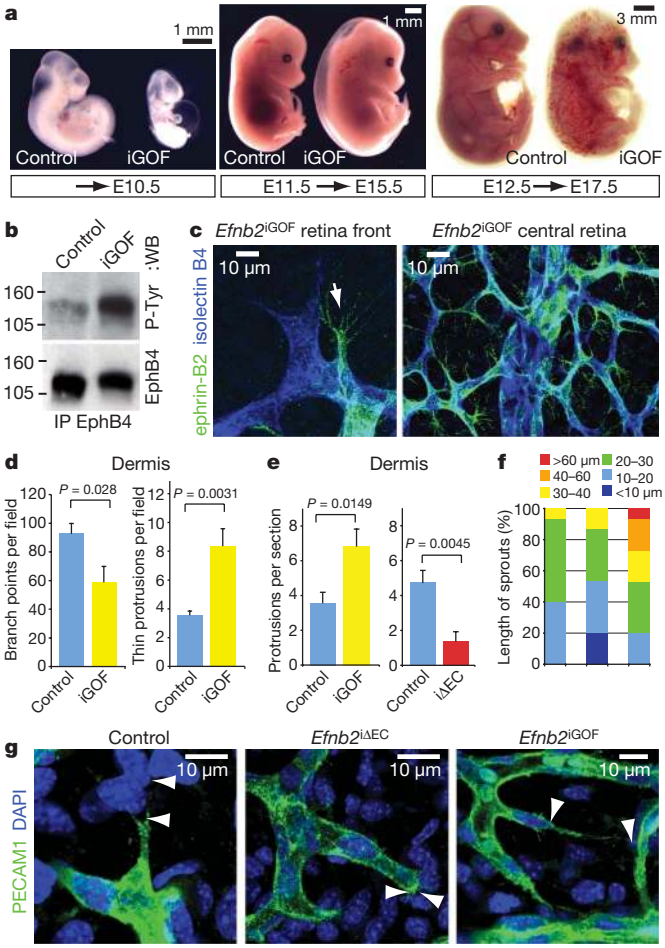

Figure 2 | Ephrin-B2 modulates endothelial cell sprouting. **a**, *Efnb2*^{iGOF} (iGOF) embryos and control littermates. Embryonic stages and induction scheme are indicated. **b**, Immunoprecipitation (IP) and western blot (WB) of EphB4 from *Efnb2*^{iGOF} (*Tie2-rtTA* × *tetO–Efnb2*) and control tissues. Phosphorylation (P-Tyr) of EphB4 is increased. Molecular masses (in kilodaltons) are indicated. **c**, CFP-ephrin-B2 (green) labels filopodia-extending endothelial cells in the tip cell region (arrow) and in the more mature plexus of the *Efnb2*^{iGOF} retina. **d**, Quantification of branch points and thin protrusions in the *Efnb2*^{iGOF} (iGOF) dermal vasculature. **e**, Quantification of ultrastructural changes in E18.5 control (Ctrl), *Efnb2*$^{i\Delta EC}$ (iΔEC) and *Efnb2*^{iGOF} (iGOF) dermal capillary endothelial cells. **f**, Length distribution of PECAM1+ sprouts in the E15.5 control and mutant dermal vasculature. **g**, Morphology of PECAM1+ (green) control and *Efnb2* mutant sprouts. Arrowheads indicate the length of filopodia. Nuclei, DAPI (blue). *P* values (**d**, **e**) were calculated using two-tailed Student's *t*-test ($n \geq 3$). Error bars, s.e.m.

blood vessel network with numerous thin endothelial connections and processes (Fig. 2d and Supplementary Fig. 6c). Many of these long sprouts and bridge-like connections appear unstable, as we regularly saw empty (collagen IV-positive but PECAM1-negative) basement membrane sleeves, a known indicator for the retraction of vessels[20] (Supplementary Figs 7 and 8). *Efnb2*$^{i\Delta EC}$ loss-of-function blood vessels also contained many empty collagen IV sleeves, which were, however, short stubs suggesting that endothelial cell sprouting had been frequently initiated and abandoned at an early stage (Supplementary Fig. 7). Accordingly, the morphology and length of PECAM1-positive sprouts correlated directly with ephrin-B2 levels. Sprouts and filopodia were short in *Efnb2*$^{i\Delta EC}$ mutants and extended in the *Efnb2*^{iGOF} dermal vasculature (Fig. 2f, g). Similarly, the ultrastructural examination of dermal capillaries confirmed that endothelial cells lacked cellular processes when ephrin-B2 expression was reduced, whereas many protrusions emerged from the *Efnb2*^{iGOF} endothelium (Fig. 2e and Supplementary Fig. 8). As a further link to endothelial cell motility, microinjection of an ephrin-B2 expression construct into individual cells within an endothelial monolayer induced migration, the dynamic extension of cellular protrusions and invasive behaviour. This process depended at least partly on EphB4 activation and was inhibited with specific kinase inhibitors (Supplementary Figs 9–13 and Supplementary Movie 3).

Ephrin-B2 regulates angiogenic growth of the blood vessel and lymphatic endothelium[11,13,21] (Supplementary Fig. 14), which both strongly rely on signalling by the receptor tyrosine kinase VEGFR3, a receptor for VEGF-C[22–24]. Indicative of a link between both signalling systems, stimulation of forward and/or reverse Eph–ephrin signalling with soluble recombinant ephrin-B2/Fc or EphB4/Fc fusion proteins led to the internalization of VEGFR3 in cultured lymphatic endothelial cells (LECs) (Fig. 3a, b). VEGF-C-induced VEGFR3 endocytosis was compromised in cultured mouse *Efnb2* knockout endothelial cells, demonstrating that this process is functionally linked to ephrin-B2 (Fig. 3d–f). Indicating a specific role of ephrin-B2 for certain receptor tyrosine kinases, the receptor for epidermal growth factor (EGF) was rapidly internalized in both control and *Efnb2* knockout cells (Supplementary Fig. 15). Moreover, ephrin-B2-deficient cells showed reduced chemotaxis towards VEGF but not other factors such as fibroblast growth factor (Supplementary Fig. 15).

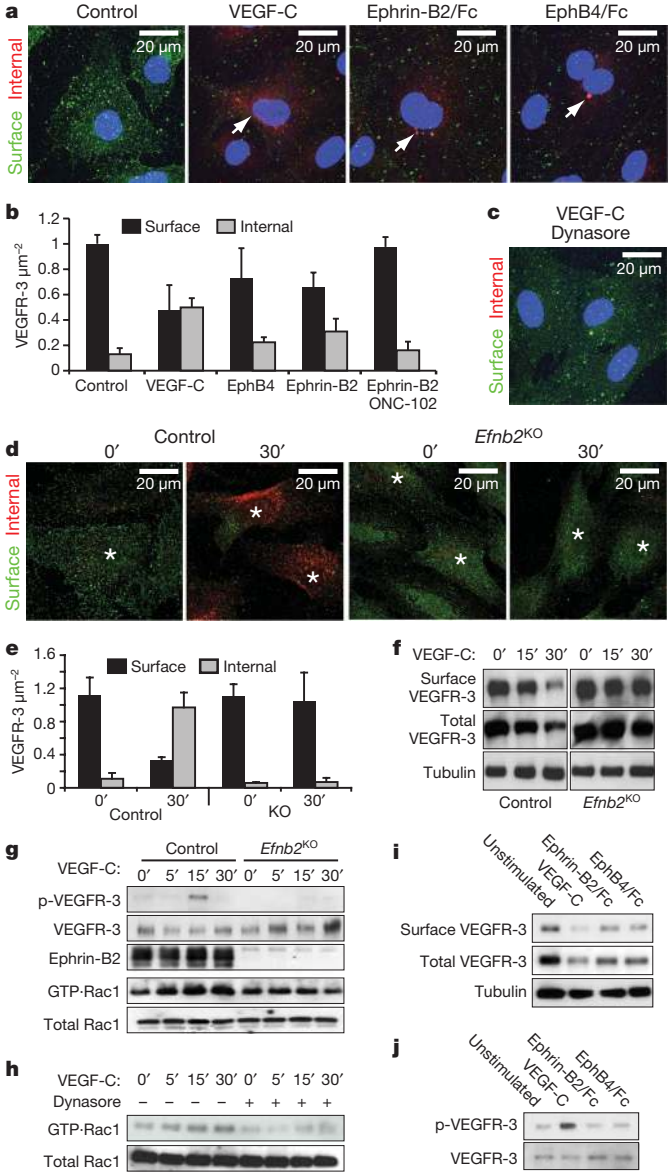

Figure 3 | VEGFR3 internalization and signalling. **a**, Immunofluorescence of cell surface (green) and internalized (red, arrows) VEGFR3 in cultured human LECs 20 min after the indicated treatments. Nuclei, DAPI (blue). **b**, Quantification shown as VEGFR3 signal per square micrometre. The effect of ephrin-B2/Fc is blocked by Eph kinase inhibition (ONC-102). **c**, Dynasore inhibits VEGF-C-induced VEGFR3 endocytosis in mouse endothelial cells. Nuclei, DAPI (blue). **d**, Endocytosed (red) and surface (green) VEGFR3 in VEGF-C-stimulated mouse control or *Efnb2* knockout endothelial cells. Asterisks mark nuclei. **e**, Quantification of VEGF-C-induced VEGFR3 internalization. **f**, Detection of surface VEGFR3 in stimulated control and *Efnb2* knockout endothelial cells by biotinylation. **g**, Induction of VEGFR3 tyrosine phosphorylation (p-VEGFR3) and activation of Rac1 (GTP·Rac1) in control and *Efnb2* knockout endothelial cells. **h**, Dynasore blocks VEGF-C-induced Rac1 activation in mouse endothelial cells. **i**, Biotinylated (surface) VEGFR3 in stimulated mouse endothelial cells. **j**, Tyrosine phosphorylation of VEGFR3 after stimulation. Error bars (**b**, **e**), s.e.m. ($n \geq 3$).

Not only internalization of VEGFR3 but also its signalling activity relies on ephrin-B2. In *Efnb2* knockout cells, VEGF-C-induced VEGFR3 tyrosine phosphorylation and activation of the small GTPase Rac1, a regulator of cell motility and protrusion formation, were markedly reduced (Fig. 3g). Likewise, phosphorylation of the serine/threonine protein kinase Akt, which promotes angiogenic behaviour[25,26], and of the mitogen-activated protein kinase Erk1/2, a signal linked to endothelial cell proliferation, were compromised (Supplementary Fig. 15). Treatment of endothelial cells with the inhibitor Dynasore, which blocks dynamin-dependent endocytosis[27], also impaired VEGF-C-induced VEGFR3 internalization and the activation of Rac1 (Fig. 3c, h).

Without VEGF-C, stimulation of endothelial cells with recombinant ephrin-B2 or EphB4 triggered VEGFR3 internalization but failed to induce appreciable activation of the receptor tyrosine kinase (Fig. 3i, j). Thus, although ephrin-B2 is indispensable for full VEGFR3 signalling, Eph–ephrin interactions alone cannot substitute for VEGF-C.

Although the exact role of ephrin-B2 in VEGFR3 endocytosis remains to be addressed, some results hint at a very transient process at the cell membrane. Co-localization of ephrin-B2 and VEGFR3 was visible on the cell surface shortly after VEGF-C stimulation, whereas there was almost no overlap inside cells (Fig. 4a and data not shown).

Ephrin-B2 is also an important regulator of VEGFR3 internalization (and presumably signalling) *in vivo*. After intraperitoneal injection of

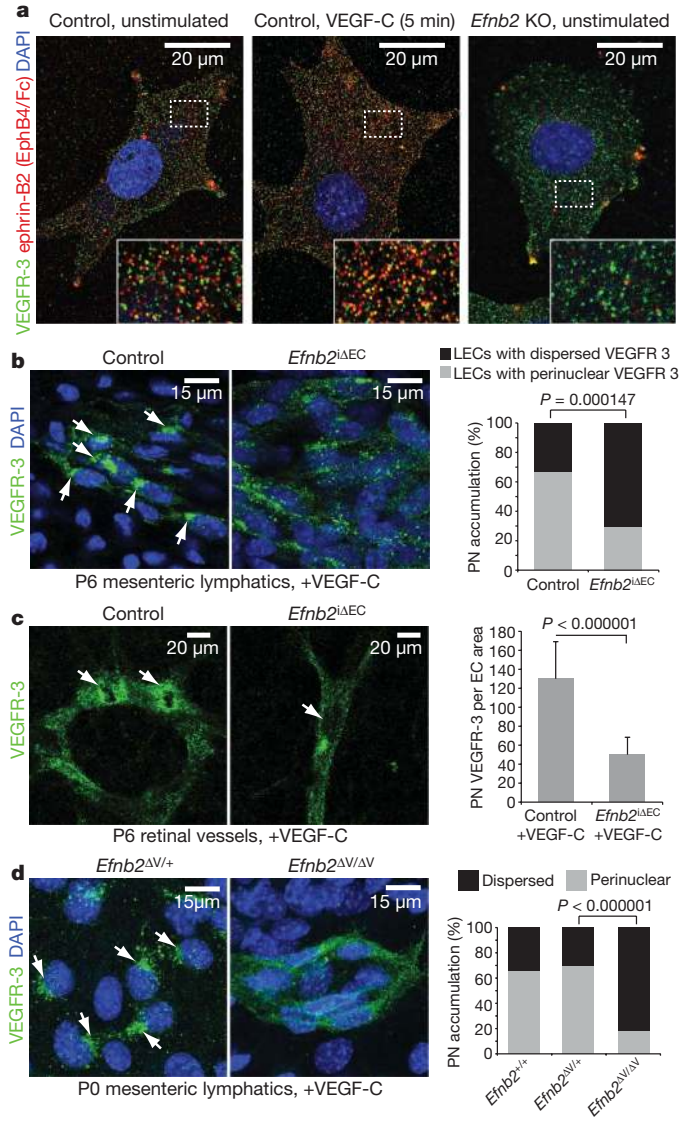

Figure 4 | Ephrin-B2 controls VEGFR3 internalization *in vivo*. **a**, Surface co-localization (yellow) of VEGFR3 (green) and ephrin-B2 (bound EphB4/Fc, red) in cultured human LECs after VEGF-C stimulation. **b**, Confocal images and quantitative analysis of VEGFR3 distribution in P6 control and *Efnb2*$^{i\Delta EC}$ mesenteric lymphatic vessels after VEGF-C injection. Arrows, perinuclear (PN) accumulation of VEGFR3 (green). Nuclei, DAPI (blue). **c**, Impaired VEGF-C-induced perinuclear accumulation of VEGFR3 (green) in *Efnb2*$^{i\Delta EC}$ retinal blood vessels. LECs, lymphatic endothelial cells. **d**, VEGF-C stimulation fails to induce VEGFR3 (green) internalization in P0 *Efnb2*$^{\Delta V/\Delta V}$ mesenteric lymphatic vessels. Nuclei, DAPI (blue). *P* values (**b**–**d**) were calculated using two-tailed Student's *t*-test. Error bars (**c**), s.e.m. ($n \geq 3$).

VEGF-C, VEGFR3 strongly accumulated in the perinuclear regions of mesenteric LECs in postnatal control but not *Efnb2*$^{i\Delta EC}$ animals (Fig. 4b and Supplementary Fig. 16). Likewise, perinuclear accumulation of VEGFR3 after intraocular injection of VEGF-C was not seen in *Efnb2*$^{i\Delta EC}$ retinal blood vessels (Fig. 4c). Consistent with the previously reported role of ephrin-B2 reverse signalling in lymphangiogenesis, VEGF-C-induced internalization of VEGFR3 was also defective in the mesenteric lymphatic vessels of newborn *Efnb2*$^{\Delta V/\Delta V}$ mutants, which lack the carboxyterminal PDZ motif and develop severe postnatal lymphangiogenesis defects[21] (Fig. 4d). Like in growing blood vessels, ephrin-B2 and EphB4 expression partly overlap in the lymphatic endothelium[21]. Thus physical interactions between LECs could lead to bi-directional Eph–ephrin signalling and thereby modulate VEGFR3 endocytosis, similar to what we are proposing for blood vessels.

As shown in the accompanying paper[28], ephrin-B2 also regulates the internalization and signalling activity of VEGFR2, a receptor tyrosine kinase that is closely related to VEGFR3, and plays a central role in the regulation of blood vessel growth. Both studies together provide compelling evidence that ephrin-B2 functions as a general modulator of the VEGF pathway in all endothelial cell types during physiological and pathological angiogenesis (Supplementary Fig. 1). We propose that this activity integrates VEGF signalling and other Eph/ephrin-controlled functions such as the regulation of cytoskeletal organization, cell motility, invasiveness and adhesion to ensure the efficient growth of blood vessels and lymphatic vessels.

METHODS SUMMARY

Loss-of-function genetics. *Cdh5-CreERT2* mice were bred into a background of animals carrying a *loxP*-flanked *Efnb2* gene[29,30] (*Efnb2*$^{lox/lox}$). Cre activity during embryogenesis was induced by three consecutive intraperitoneal injections of pregnant females at days 11.5, 12.5 and 13.5 post coitum with 100 μl tamoxifen solution (Sigma, T5648; 10 mg ml^{-1}; generated by diluting a 10× tamoxifen stock in 100% ethanol with peanut oil). To induce Cre activity in newborn mice, three consecutive intraperitoneal tamoxifen (1 mg ml^{-1} in ethanol/peanut oil) injections of 50 μl were given on postnatal day (P)1, P2 and P3. The phenotypes of mutant mice were analysed at postnatal stages P5 or P6, as indicated. Littermate animals were used as control.

Generation of *Efnb2*^{iGOF} mice. A DNA encoding enhanced CFP and a Flag epitope were inserted in frame into the unique ClaI restriction site within the murine *Efnb2* cDNA. EphB4 binding to this fusion protein was verified by transient expression in cultured cells. *CFP–ephrin-B2* was inserted into the plasmid pUHD10-3 (http://www.zmbh.uni-heidelberg.de/bujard/reporter/pUHD10-3.html) containing a tetracycline-responsive promoter. Transgenic founders (tetO-*Efnb2*) were generated by pronuclear injection and tested in combination with *vascular endothelial (VE)-cadherin-tTA*[19] or *Tie2-rtTA*[31] transgenics. Both driver lines gave very similar results during embryonic development, but only *VE-cadherin-tTA* is expressed in both lymphatic and blood vessel endothelial cells.

Specificity. No defects were observed in *VE-cadherin-tTA*, *Tie2-rtTA*, *CFP-ephrin-B2* or *CreERT2* single transgenic animals or in *CreERT2/+ Efnb2*$^{lox/lox}$ animals that had not received tamoxifen.

Ethical review. All animal experiments were performed in compliance with the relevant laws and institutional guidelines and were approved by local animal ethics committees.

Full Methods and any associated references are available in the online version of the paper at www.nature.com/nature.

Received 25 October 2009; accepted 2 March 2010.
Published online 5 May; corrected 27 May 2010 (see full-text HTML version for details).

1. Adams, R. H. & Alitalo, K. Molecular regulation of angiogenesis and lymphangiogenesis. *Nature Rev. Mol. Cell Biol.* **8,** 464–478 (2007).
2. Gerhardt, H. & Betsholtz, C. How do endothelial cells orientate? *Experientia*, Suppl. 94, 3–15 (2005).
3. Klagsbrun, M. & Eichmann, A. A role for axon guidance receptors and ligands in blood vessel development and tumor angiogenesis. *Cytokine Growth Factor Rev.* **16,** 535–548 (2005).
4. Arvanitis, D. & Davy, A. Eph/ephrin signaling: networks. *Genes Dev.* **22,** 416–429 (2008).
5. Egea, J. & Klein, R. Bidirectional Eph-ephrin signaling during axon guidance. *Trends Cell Biol.* **17,** 230–238 (2007).
6. Poliakov, A., Cotrina, M. & Wilkinson, D. G. Diverse roles of eph receptors and ephrins in the regulation of cell migration and tissue assembly. *Dev. Cell* **7,** 465–480 (2004).
7. Pasquale, E. B. Eph receptor signalling casts a wide net on cell behaviour. *Nature Rev. Mol. Cell Biol.* **6,** 462–475 (2005).
8. Lawson, N. D. & Weinstein, B. M. Arteries and veins: making a difference with zebrafish. *Nature Rev. Genet.* **3,** 674–682 (2002).
9. Lamont, R. E. & Childs, S. MAPping out arteries and veins. *Sci. STKE* **2006,** pe39 (2006).
10. le Noble, F. *et al.* Flow regulates arterial–venous differentiation in the chick embryo yolk sac. *Development* **131,** 361–375 (2004).
11. Wang, H. U., Chen, Z. F. & Anderson, D. J. Molecular distinction and angiogenic interaction between embryonic arteries and veins revealed by ephrin-B2 and its receptor Eph-B4. *Cell* **93,** 741–753 (1998).
12. Gerety, S. S., Wang, H. U., Chen, Z. F. & Anderson, D. J. Symmetrical mutant phenotypes of the receptor EphB4 and its specific transmembrane ligand ephrin-B2 in cardiovascular development. *Mol. Cell* **4,** 403–414 (1999).
13. Adams, R. H. *et al.* Roles of ephrinB ligands and EphB receptors in cardiovascular development: demarcation of arterial/venous domains, vascular morphogenesis, and sprouting angiogenesis. *Genes Dev.* **13,** 295–306 (1999).
14. Shin, D. *et al.* Expression of ephrinB2 identifies a stable genetic difference between arterial and venous vascular smooth muscle as well as endothelial cells, and marks subsets of microvessels at sites of adult neovascularization. *Dev. Biol.* **230,** 139–150 (2001).
15. Gale, N. W. *et al.* Ephrin-B2 selectively marks arterial vessels and neovascularization sites in the adult, with expression in both endothelial and smooth-muscle cells. *Dev. Biol.* **230,** 151–160 (2001).
16. Davy, A. & Soriano, P. Ephrin-B2 forward signaling regulates somite patterning and neural crest cell development. *Dev. Biol.* **304,** 182–193 (2007).
17. Taylor, A. C., Murfee, W. L. & Peirce, S. M. EphB4 expression along adult rat microvascular networks: EphB4 is more than a venous specific marker. *Microcirculation* **14,** 253–267 (2007).
18. Zhu, Z., Zheng, T., Lee, C. G., Homer, R. J. & Elias, J. A. Tetracycline-controlled transcriptional regulation systems: advances and application in transgenic animal modeling. *Semin. Cell Dev. Biol.* **13,** 121–128 (2002).
19. Sun, J. F. *et al.* Microvascular patterning is controlled by fine-tuning the Akt signal. *Proc. Natl Acad. Sci. USA* **102,** 128–133 (2005).
20. Baluk, P., Hashizume, H. & McDonald, D. M. Cellular abnormalities of blood vessels as targets in cancer. *Curr. Opin. Genet. Dev.* **15,** 102–111 (2005).
21. Makinen, T. *et al.* PDZ interaction site in ephrinB2 is required for the remodeling of lymphatic vasculature. *Genes Dev.* **19,** 397–410 (2005).
22. Tammela, T. *et al.* Blocking VEGFR-3 suppresses angiogenic sprouting and vascular network formation. *Nature* **454,** 656–660 (2008).
23. Tammela, T., Enholm, B., Alitalo, K. & Paavonen, K. The biology of vascular endothelial growth factors. *Cardiovasc. Res.* **65,** 550–563 (2005).
24. McColl, B. K., Stacker, S. A. & Achen, M. G. Molecular regulation of the VEGF family–inducers of angiogenesis and lymphangiogenesis. *APMIS* **112,** 463–480 (2004).
25. Zachary, I. & Gliki, G. Signaling transduction mechanisms mediating biological actions of the vascular endothelial growth factor family. *Cardiovasc. Res.* **49,** 568–581 (2001).
26. Olsson, A. K., Dimberg, A., Kreuger, J. & Claesson-Welsh, L. VEGF receptor signalling – in control of vascular function. *Nature Rev. Mol. Cell Biol.* **7,** 359–371 (2006).
27. Macia, E. *et al.* Dynasore, a cell-permeable inhibitor of dynamin. *Dev. Cell* **10,** 839–850 (2006).
28. Sawamiphak, S. *et al.* Ephrin-B2 regulates VEGF-R2 function in developmental and tumour angiogenesis. *Nature* doi:10.1038/nature08995 (this issue).
29. Grunwald, I. C. *et al.* Hippocampal plasticity requires postsynaptic ephrinBs. *Nature Neurosci.* **7,** 33–40 (2004).
30. Foo, S. S. *et al.* Ephrin-B2 controls cell motility and adhesion during blood-vessel-wall assembly. *Cell* **124,** 161–173 (2006).
31. Deutsch, U. *et al.* Inducible endothelial cell-specific gene expression in transgenic mouse embryos and adult mice. *Exp. Cell Res.* **314,** 1202–1216 (2008).

Supplementary Information is linked to the online version of the paper at www.nature.com/nature.

Acknowledgements We thank R. Benedito, I. Schmidt, S. Hoffmann, I. Rosewell, S.M. Kuijper, F. Gisler and N. Hostettler for their help, N. Copeland and A. Eichmann for information and reagents, P. Chambon for the CreERT2 cDNA, A.L. Bermange, J.D. Leslie and J. Lewis for help with zebrafish experiments, and A. Acker-Palmer for discussions and for reading the manuscript. Cancer Research UK, the Max-Planck-Society, the German Research Foundation (programmes SFB 629 and SPP 1190) and the EMBO LTF programme provided funding.

Author Contributions Y.W., M.E.P., M.N., C.D.N. and R.H.A. designed experiments. Y.W., M.E.P. and T.S.S. characterized mouse mutants. M.L.B. and A.S. performed zebrafish experiments, M.L.B. microinjection assays and M.N. all other cell culture experiments. A.D., U.D., L.E.B., S.A. and T.M. generated mouse mutants or lines, U.L. and A.B. the EphB4 inhibitors. Y.W., M.N., M.E.P. and R.H.A. wrote the manuscript.

Author Information Reprints and permissions information is available at www.nature.com/reprints. The authors declare competing financial interests: details accompany the full-text HTML version of the paper at www.nature.com/nature. Correspondence and requests for materials should be addressed to R.H.A. (ralf.adams@mpi-muenster.mpg.de).

METHODS

Loss-of-function genetics. *Cdh5-CreERT2* mice were bred into a background of animals carrying a *loxP*-flanked *Efnb2* gene[29,30] (*Efnb2*$^{lox/lox}$). Cre activity during embryogenesis was induced by three consecutive intraperitoneal injections of pregnant females at days 11.5, 12.5 and 13.5 post coitum with 100 µl tamoxifen solution (Sigma, T5648; 10 mg ml^{-1}; generated by diluting a 10× tamoxifen stock in 100% ethanol with peanut oil). To induce Cre activity in newborn mice, three consecutive intraperitoneal tamoxifen (1 mg ml^{-1} in ethanol/peanut oil) injections of 50 µl were given on postnatal day (P)1, P2 and P3. The phenotypes of mutant mice were analysed at postnatal stages P5 or P6, as indicated. Littermate animals were used as control.

Inducible *Efnb2* overexpression. A DNA encoding enhanced CFP and a Flag epitope were inserted in frame into the unique ClaI restriction site within the murine *Efnb2* cDNA. EphB4 binding to this fusion protein was verified by transient expression in cultured cells. *CFP–ephrin-B2* was inserted into the plasmid pUHD10-3 (http://www.zmbh.uni-heidelberg.de/bujard/reporter/pUHD10-3.html) containing a tetracycline-responsive promoter. Transgenic founders (tetO-*Efnb2*) were generated by pronuclear injection and tested in combination with *VE-cadherin-tTA*[19] or *Tie2-rtTA*[31] transgenics. Both driver lines gave very similar results during embryonic development, but only *VE-cadherin-tTA* is expressed in both lymphatic and blood-vessel endothelial cells.

In *Tie2-rtTA* mice, ephrin-B2 expression was triggered by adding 2 mg ml^{-1} doxycycline hydrochloride (Sigma, D9891) and 3% sucrose to the drinking water of pregnant females from day 11.5 or 12.5 post coitum onwards. To suppress overexpression transiently in the *VE-cadherin-tTA* background, pregnant females were given tetracycline water (2% sucrose in tap water containing 0.1% tetracycline (Sigma, T3258, dissolved in 50 ml absolute ethanol) from days E0.5 to E10.5. Tetracycline water was changed to normal drinking water on E11.5 to allow gene overexpression. Embryos were collected and analysed at E15.5 or E18.5, respectively. For postnatal studies, tetracycline was administered from the day of plug until E15.5, and pups were killed for analysis at P6. All *in vivo* gain-of-function results shown were obtained with *VE-cadherin-tTA* × *tetO-Efnb2* transgenics.

Generation of PAC transgenic mice. The PAC library RPCI21 (Geneservice) containing 129/SvevTACfBr mouse spleen genomic DNA in a pPAC4 vector[32] was screened by filter hybridization with radioactive mouse *Cdh5* (VE-cadherin) probes. A cDNA encoding tamoxifen-inducible Cre recombinase[33] followed by a polyadenylation signal sequence and an FRT-flanked ampicillin resistance cassette was introduced by recombineering[34] into the start codon of *Cdh5* in PAC clone 353-G15. After Flp-mediated excision of the ampicillin resistance cassette in bacteria, the resulting constructs were validated by PCR analysis and used in circular form for pronuclear injection into fertilized mouse oocytes. Founders, identified by PCR genotyping, were screened by timed matings with *ROSA26R Cre* reporter animals[35]. Cre activity was induced by three consecutive intraperitoneal injections of pregnant females at days 11.5, 12.5 and 13.5 post coitum with 100 µl tamoxifen solution (Sigma, T5648; 10 mg ml^{-1}; generated by diluting a 10 × tamoxifen stock in 100% ethanol with peanut oil). For studies in adult mice, 10 mg tamoxifen slow-release pellets (Innovative Research of America) were subcutaneously implanted into *CreERT2*/+ *ROSA26R*/+ double heterozygous animals, which were killed after 21 days. Dissected embryos or adult tissues were analysed by whole-mount β-galactosidase staining.

Specificity. No defects were observed in *VE-cadherin-tTA*, *Tie2-rtTA*, *CFP-ephrin-B2* or *CreERT2* single transgenic animals or in *CreERT2*/+ *Efnb2*$^{lox/lox}$ animals that had not received tamoxifen.

Ethical review. All animal experiments were performed in compliance with the relevant laws and institutional guidelines and were approved by local animal ethics committees.

Detection of β-galactosidase activity by X-gal staining. Whole embryos or tissues were dissected and fixed in X-gal fixation solution (0.2% glutaraldehyde, 5 mM EGTA, 2 mM $MgCl_2$ in PBS) at room temperature for 15–20 min, and then washed in wash buffer (2 mM $MgCl_2$, 0.02% NP-40 in PBS) for 3 × 5 min. Samples were stained in X-gal staining buffer (1.64 mg ml^{-1} potassium ferricyanide, 2.12 mg ml^{-1} potassium ferrocyanide, 1 mg ml^{-1} X-gal in wash buffer) at 37 °C with gentle rocking until the desired staining level had been achieved. The embryos or tissues were washed in PBS several times at room temperature and then post-fixed in 4% PFA for 5 min at room temperature. Samples were briefly washed in PBS and photographed.

Isolation and culture of mouse endothelial cells. Heart and lung were taken from adult *Efnb2*$^{lox/lox}$ animals carrying the *H-2Kb-tsA58* allele for conditional expression of temperature-sensitive SV40 large T[36] and transferred into ice-cold PBS. Tissues were washed twice with ice-cold PBS-PenStrep (400 ml endotoxin-free PBS containing 5 ml penicillin/streptomycin) and cut into small pieces. Tissue pieces were washed twice more with ice-cold PBS-PenStrep and incubated in 10 ml 0.25% collagenase (made by diluting 2.5% collagenase in PBS containing 3 mM $CaCl_2$ with PBS) for 30 min at 37 °C. After passage through a 100-µm cell strainer, tissues were collected and digested in 1 U dispase per millilitre, 0.25% collagenase for 3 h at 37 °C. The digested tissues were passed through a 100-µm cell strainer and the eluted cell suspension was collected in a Falcon tube. Tissue fragments were collected into a 2-ml Eppendorf tube, washed with 300 µl 10% FCS in DMEM, passed through the cell strainer again and the flow-through was combined with the previously saved cell suspension. The cell strainer was washed several times with 1 ml 10% FCS in DMEM and the flow-through was again collected. All saved suspensions were combined and spun for 5 min at 210*g* at room temperature. The supernatant was aspirated and the precipitated cells were washed once with 10% FCS in DMEM. Cells were cultured in a collagen- (Becton Dickinson, 5 µg cm^{-2} in PBS) coated T75 cell culture flask (Corning) containing Medium200 (Cascade Biologics) at 37 °C and 5% CO_2 and the medium was changed next day. After 2–3 days, Medium200 was changed to the medium for immortalized endothelial cells (400 ml DMEM, 50 ml FCS, 3 mM L-glutamine, 1 mM MEM sodium pyruvate, 1 × non-essential amino acids, 5 ml penicillin/streptomycin, 50 µl recombinant human VEGF-A165 at a concentration of 50 µg ml^{-1} in PBS, 25 µl recombinant murine interferon-γ at a concentration of 10^3 U µl^{-1}) and the cells were incubated at 33 °C and 5% CO_2.

Endothelial cells were isolated from the cells in three confluent T75 cell culture flasks using CELLection Biotin Binder Kit (Dynal) and biotinylated anti-PECAM1 antibody (Becton Dickinson) according to the manufacturer's instructions. Cells were incubated at 37 °C in the absence of interferon-γ for 72 h before experimental analysis.

Immunoprecipitation. Tissue lysates from embryonic organs were prepared in PLC buffer (50 mM HEPES pH 7.0, 150 mM NaCl, 10% Glycerol, 0.1% Triton X-100, 1.5 mM $MgCl_2$, 1 mM EGTA, 1% NP-40, 100 mM NaF, 10 mM $Na_4P_2O_7$, 1 mM Na_3VO_4, protease inhibitor cocktail (Sigma, P2714, 1:100)) using a tissue homogenizer (Ultra-Turrax, IKA) and incubated for 30 min on ice. Tissue debris was removed by centrifugation. Total protein lysate (1–2 mg) was precleared with uncoupled protein A or G beads and incubated with antibody-coupled beads for 1 h at 4 °C. After several washes with PLC buffer, precipitated proteins were resuspended in Laemmli loading buffer and analysed by SDS–polyacrylamide gel electrophoresis and western blot.

For signalling studies in cultured cells, control (*Efnb2*$^{lox/lox}$) and *Efnb2* knockout cells, or human LECs (Lonza) were seeded at a density of 3.0×10^5 in 6-cm dishes and incubated for 24 h. Before stimulation, cells were deprived of serum for 24 h. For the EphB4 inhibitor treatment, serum-deprived cells were treated with 10 µM of ONC-102 for 45 min. Cells were then incubated in serum-free growth medium containing 2 µg ml^{-1} EphB4/Fc, 2 µg ml^{-1} ephrin-B2/Fc, 2 µg ml^{-1} hIgG/Fc (R&D Systems), or 100 ng ml^{-1} of VEGF-C (ReliaTech) at 37 °C for the indicated times, collected with 100 µl of 1 × SDS sample buffer and subjected to immunoblotting with phospho-AKT (Ser 473) antibody (Cell Signaling), phospho-p44/42 MAPK antibody (Cell Signaling), AKT antibody (Cell Signaling), or p44/42 MAPK antibody (Cell Signaling).

For the detection of phosphorylated VEGFR3, VEGF-C-stimulated control and *Efnb2* knockout cells were lysed in 0.2 ml lysis buffer (25 mM Tris-HCl (pH 7.5), 150 mM NaCl, 5 mM EDTA/NaOH (pH 8.5), 1% NP-40, 100 mM NaF, 10 mM $Na_4P_2O_7$, 1 mM Na_3VO_4, protease inhibitor cocktail (Sigma, P2714, 1:100)). After centrifugation, supernatants were collected and were incubated with 5 µg anti-FLT4 antibody (R&D Systems) for 2 h at 4 °C. Samples were incubated with Protein G Sepharose beads (GE Healthcare) for 60 min at 4 °C and precipitated by centrifugation. Immunoprecipitated proteins were separated in 7% SDS–polyacrylamide gel electrophoresis and subjected to western blotting analysis with anti-phosphotyrosine antibody (4G10, Cell Signaling).

Eph kinase inhibitors. ONC-101 and ONC-102 were identified by Oncalis AG Biotech Center Zürich, Switzerland. The synthesis of these compounds is described in the Supplementary Information. Values for the half-maximum inhibitory concentration were determined by *in vitro* kinase assay with radiolabelled [γ-^{32}P]ATP. Profiling of inhibitor binding to different kinases was performed by Ambit Biosciences.

Staining of tissues, sections and cells. The isolation, processing and staining of skin whole-mount samples and the detection of ephrin-B2 and EphB4 on paraffin sections have been published previously[30]. Antibodies for whole-mount staining were rabbit anti-GFP (Molecular Probes, dilution 1:500), rabbit anti-collagen IV (Chemicon, 1:200), rat monoclonal anti-PECAM1 (Pharmingen, clone MEC13.3m, 1:200), rat monoclonal anti-endomucin (clone V.7C7AK, 1:100)[37], mouse anti-αSMA-Cy3 (Sigma Aldrich, clone 1A4, 1:400) and rabbit anti-Prox1 (Abcam, 1:400). Eph/ephrin molecules were detected in paraffin sections with goat anti-ephrin-B2 (1:100) and anti-EphB4 (1:200) antibodies (R&D Systems). Secondary antibodies were goat anti-rat IgG, goat anti-rabbit IgG conjugated to Alexa-488 or Alexa-546 (Molecular Probes), or Cy3-conjugated goat anti-rat IgG (Jackson, 1:500). Images were recorded with a Leica DM IRBE

microscope and Openlab software (Improvision) or a Zeiss LSM510 Meta confocal microscope.

Intestines were dissected from P0 or P6 pups and fixed in 4% PFA for 10 min on ice before mesenteries were dissected and fixed for a further 1 h on ice. Tissues were washed three times with PBT (0.1% Tween-20 in PBS) and permeabilized/blocked overnight in blocking buffer (1% BSA, 1% donkey serum, 0.5% Tween-20 in PBS) overnight at 4 °C with gentle rocking. Goat anti-VEGFR3 antibody (R&D Systems, AF 743, 1:100) or rabbit anti-Prox1 antibody (ReliaTech, 102-PA32AG, 1:500) were incubated in 0.5% BSA, 0.5% donkey serum and 0.25% Tween-20 in PBS and applied overnight at 4 °C. After five times PBT washings mesenteries were incubated with Alexa-Fluor-coupled secondary antibodies (Invitrogen, 1:500) overnight at 4 °C. Nuclei were stained using DAPI (Sigma, D9542) and mesenteries were flat-mounted using Fluromount-G (SouthernBiotech, 0100-01).

For retina staining, eyes were dissected and fixed in 4% PFA for 2 h at room temperature or on ice. Retinas were dissected and permeabilized and blocked in 1% BSA (Sigma, A4378-25G) and 0.3% Triton X-100 overnight at 4 °C with gentle rocking. Next, retinas were washed three times in Pblec buffer (1 mM $CaCl_2$, 1 mM $MgCl_2$, 1 mM $MnCl_2$ and 1% Triton X-100 in PBS) and incubated with biotinylated isolectin B4 (Vector, B-1205, *Griffonia simlicifolia* lectin I) diluted 1:25 in Pblec, overnight at 4 °C with gentle rocking. Retinas were washed five times in 0.5% BSA and 0.15% Triton X-100 and incubated with Alexa-Fluor-coupled streptavidin (Molecular Probes, 1:100) in blocking buffer for 2 h at room temperature. Primary antibodies diluted in blocking buffer were applied overnight at 4 °C: Alexa-488-coupled rabbit anti-GFP (Molecular Probes, A21311, 1:500) and goat anti-VEGFR3 (R&D Systems, AF 743, 1:50). After washing steps, retinas were incubated with appropriate Alexa-Fluor-coupled secondary antibodies (Invitrogen, 1:500) in blocking buffer for 2 h at room temperature. Nuclei were stained with TO-PRO-3 (Invitrogen, T3605). Retinas were flat-mounted using Fluromount-G (SouthernBiotech, 0100-01).

Retinas to be stained for EphB4 were dissected from eyes fixed in 4% PFA for 2 h on ice. Retinas were blocked and permeabilized overnight in TNB 0.2% Triton X-100 containing 1 mM Tris-HCl, pH 7.4, 15 mM NaCl and 0.5% blocking reagent (Roche, 11096176001). Goat anti-EphB4 antibodies (R&D Systems, AF446, 1:50) diluted in TNB 0.2% Triton X-100 were applied overnight at 4 °C. Next, retinas were washed six times in PBS and 0.2% TritonX-100 and incubated with secondary antibodies. Afterwards, retinas were processed for isolectin B4 staining, refixed for 30 min in 4% PFA at room temperature and mounted as described above.

For the labelling of proliferating cells, P6 pups received intraperitoneal injections with 5-bromo-2′ deoxyuridine (Invitrogen, B23151, 300 μg BrdU dissolved in 100 μl PBS). After 2.5 h, pups were killed and eyes were dissected and fixed for 2 h at room temperature. After isolectin B4 staining, retinas were refixed in 4% PFA for 30 min at room temperature and incubated in 50% formamide, 1 × SSC solution at 65 °C for 1 h. Retinas were then incubated in 2 N HCl at 37 °C for 30 min and neutralized with 0.1 M Tris-HCl (pH 8.0) twice for 10 min each. After washing with PBS, retinas were blocked for 2 h at room temperature, and monoclonal mouse anti-BrdU antibodies (Becton Dickinson, 347580, 1:50) diluted in blocking buffer were incubated overnight at 4 °C with gentle rocking. Next, staining and mounting was performed as described above.

Electron microscopic examination of embryonic skin samples was performed as published previously[30].

To visualize VEGFR3 and ephrin-B2 on the cell surface of cultured endothelial cells, control (*Efnb2*$^{lox/lox}$) and *Efnb2* knockout cells were fixed with 4% PFA, 4% sucrose in PBS on ice for 10 min, incubated with blocking solution containing 2% (w/v) BSA and 4% (w/v) donkey serum (Abcam) for 10 min at room temperature. Primary antibody (anti-FLT4 antibody, R&D Systems) and 5 μg ml^{-1} of EphB4/Fc (R&D Systems) were incubated with blocking solution for 1 h at room temperature. After washing with PBS, cells were incubated with Alexa-Fluor-488-conjugated secondary antibody (Invitrogen) and Cy3-conjugated anti-human IgG Fc (Jackson Laboratories) for 1 h at room temperature.

Antibody feeding and receptor internalization assays. To analyse the internalization of VEGFR3 *in vitro*, human LECs (Lonza) or *Efnb2*$^{lox/lox}$ and *Efnb2* knockout cells were incubated with blocking solution containing 2% (w/v) BSA and 4% (w/v) donkey serum (Abcam) for 10 min at 37 °C. Primary antibody (anti-FLT4, R&D Systems, diluted 1:40 in blocking solution) was added and incubated with the cells for 20 min at 37 °C. After washing with PBS, cells were incubated in serum-free growth medium containing 2 μg ml^{-1} EphB4/Fc, 2 μg ml^{-1} ephrin-B2/Fc, 2 μg ml^{-1} Fc (R&D Systems) or 100 ng ml^{-1} VEGF-C at 37 °C for 30 min, and fixed with 4% PFA and 4% sucrose in PBS on ice for 30 min. The detection of VEGFR3 on the cell surface was done by incubation with Alexa-Fluor-488-conjugated secondary antibody (Invitrogen, 1:100) for 2 h at room temperature. After three washes of 5 min in PBS, cells were permeabilized for 30 min with ice-cold PBS containing 0.2% Triton-X100, 2% (w/v) BSA and 4% donkey serum. Alexa-Fluor-546-conjugated secondary antibody (Invitrogen, 1:400) was incubated with cells for 1 h at room temperature to visualize internalized receptors. Quantitative measurements were performed with Volocity software (Improvision). The number of VEGFR3 signals in 1 μm^2 was calculated from at least ten cells from each group; three independent experiments were performed.

Cell surface biotinylation was performed on *Efnb2*$^{lox/lox}$ and *Efnb2* knockout cells (in 100-mm diameter dishes). Surface receptors were labelled with 0.5 mg ml^{-1} sulpho-NHS-LC-biotin (Thermo Scientific) according to the manufacturer's instructions. After quenching of excess biotin with 100 mM glycine in PBS, the cells were dissolved in 0.8 ml lysis buffer (25 mM Tris-HCl (pH 7.5), 150 mM NaCl, 5 mM EDTA-NaOH (pH 8.5) 1% NP-40, 100 mM NaF, 10 mM $Na_4P_2O_7$, 1 mM Na_3VO_4 and protease inhibitor cocktail (Sigma, P2714, 1:100)). The lysates were precipitated with streptavidin agarose beads (Invitrogen), and the precipitates were analysed by immunoblot with anti-VEGFR3 antibody (eBioscience) or EGFR antibody (Abcam).

VEGFR3 internalization *in vivo* and *ex vivo*. For the stimulation of VEGFR3 in retinal endothelial cells, eyes were isolated and immediately injected with 500 ng VEGF-C (ReliaTech, 300-079). Fluid (1 μl) was injected into the vitreous humour trough the optic disc with a microinjector (Pneumatic PicoPump, PV820) and fine glass capillaries with filament (World Precision Instruments, 1.0 mm, 3IN), which had been generated with a pulling machine (Sutter Instrument Co. model P-97). The contralateral eye was injected with 1 μl PBS (vehicle control). The eyes were transferred in 0.9% NaCl solution and incubated for 30 min at room temperature. Next, eyes were fixed in 4% PFA for 2 h on ice and immunostained as described above.

For the analysis of VEGFR3 localization in lymphatic vessels, P0 mutant and control mice were injected intraperitoneally using a 30-gauge needle with a VEGF-C solution (300 ng VEGF-C dissolved in 30 μl PBS) or PBS only. P6 mutant or control mice were injected with 500 ng VEGF-C dissolved in 80 μl PBS. After 1 h, the pups were killed and mesenteries were processed for immunostaining as described above.

Cell culture and microinjection. Human umbilical cord venous or arterial endothelial cells (TCS Cellworks) were cultured in endothelial serum-free medium (Gibco) containing 2% FCS, EGF, basic fibroblast growth factor, heparin and gentamycin and were used from passage 4–8. Cells were plated on attachment factor-coated (TCS Cellworks) glass coverslips for 2–5 days (high density) before use. Cell nuclei were microinjected with pRK5ephrin-B2 or pRK5 alone (control) at a concentration of 200 μg ml^{-1} in PBSA and injection marker (2 mg ml^{-1} lysinated biotin dextran, Molecular Probes). Microscope images were collected (one frame every 30 s) for time-lapse analysis within 10 min of cell microinjection under an inverted microscope using a ×40 phase-contrast objective, an Orca-ER camera (Hamamatsu) and Openlab (Improvision) software. Cells were maintained at 37 °C and 5% CO_2 during recording. After time-lapse, cells were fixed and stained to identify microinjected cells. Microinjection with EphB4 was used to validate the Eph kinase inhibitors ONC-101 and ONC-102.

Matrigel assay. Matrigel (BD Biosciences) was thawed on ice and dispersed on coverslips in 24-well plates (40 μl per well) and allowed to polymerize for 30 min at 37 °C. Immortalized mouse endothelial cells were seeded on the matrigel at the density of 2.5 × 10^4 cells per well. Cells were incubated for 15–16 h at 37 °C and 5% CO_2 and then subjected to antibody staining.

Zebrafish injection, immunofluorescence and time-lapse imaging. Morpholino oligonucleotides (*efnb2a* MO-1 (translation blocking): ATATCT CCACAAAGAGTCGCCCATG; *efnb2a* MO-2 (splice blocking): TTGCCGC CTCGCGCACTTACTTGT; *efnb2a*-MO(5mut): ATATgTCCAgAAAcAGTCcC CgATG) were diluted in Danieau buffer containing 0.05% phenol red to a concentration of 0.4 mM. Two- to four-cell stage *fli1*–EGFP embryos[38] were injected with 2 nl of morpholino oligonucleotide dilution, kept in E2 medium (15 mM NaCl, 0.5 mM KCl, 1 mM $CaCl_2$, 1 mM $MgSO_4$, 0.15 mM KH_2PO_4, 0.05 mM Na_2HPO_4; pH 7.0–7.5) and incubated at 28 °C until imaging. Morphant and control embryos were carefully stage-matched. The gross morphology of the injected fish appeared normal with the indicated morpholino oligonucleotide concentrations. After removal of the chorion, embryos were anaesthetized with 200–300 μg ml^{-1} tricaine (Sigma) for 1 min and mounted on a 22 mm × 50 mm cover glass with 0.3% low melting point agarose (Sigma A9414) in E2 media supplemented with tricaine. EGFP-derived fluorescence was observed with a Leica TCS SP5 confocal microscope with ×20 objective at room temperature. Images of two intersegmental vessels located near the end of yolk extension were captured every minute for 1 h. Time-lapse movies consisting of 61 frames are provided as Supplementary Movies.

For anti-ephrin-B2a immunofluorescence, morpholino-oligonucleotide-injected or control embryos at 24 hours post-fertilization were fixed with 4% PFA/PBS overnight at 4 °C, followed by three washes with PBS supplemented with 0.5% Triton X-100 (PBST). Yolk of the embryos was removed mechanically.

Embryos were digested with proteinase K at 10 μg ml^{-1} for 3 min, washed with PBST and re-fixed with 4% PFA/PBS for 10 min, at room temperature. Embryos were embedded in 4% low melting point agarose/PBS. Sections (200 μm) were prepared using a VT1200S Leica vibratome, followed by permeabilization with PBS containing 0.3% Triton X-100 and 0.1% Tween-20 (PTT) and blocking with PBS containing 4% BSA (PBT) for 1 h at 4 °C. Goat anti-ephrin-B2a antibodies (R&D Systems, AF1088), diluted in PBT were incubated overnight, at 4 °C. Sections were washed five times in PBS containing 0.3% Triton X-100 (PT) and secondary, fluorescent-conjugated, antibodies (Alexa-Fluor-488-labelled donkey anti-goat IgG, Molecular Probes) were incubated overnight, at 4 °C. After five washes in PT, sections were mounted on microscope slides (Carl Roth, H870) with Fluoromount-G (SouthernBiotech, 0100-01).

Quantification and image processing. Volocity (Improvision), Photoshop CS and Illustrator CS (Adobe) software were used for image processing in compliance with the *Nature* 'guide for digital images'. Data are based on at least three independent experiments or three mutant and control animals for each stage and result shown.

Analysis of branching points, tip cells, filopodia and endothelial cell area was performed with Volocity software (Improvision). Tip cells were defined as sprouting endothelial cells with filopodial extensions. The angiogenic front in the retina was defined as the line connecting the basis of the sprouting endothelial cells. The sprouts were defined as protrusive endothelial cells above the angiogenic front line. All quantifications were done using high-resolution confocal images and thin *z*-section of the sample.

Analysis of VEGFR3 distribution in endothelial cells after VEGF-C stimulation was performed in LECs of mesenteries from P0 or P6 treated pups and in blood endothelial cells from P6 retinas. All quantifications were done using high-resolution confocal images.

The distribution of VEGFR3 was analysed in 140–200 LECs in three mesenteries per group. The ratios of cells with strong perinuclear VEGFR3 to the total number of cells with strong perinuclear, weak perinuclear or dispersed VEGFR3 were calculated and averaged.

The cells with strong perinuclear VEGFR3 distribution in retinal endothelial cells were counted in 21 fields (three retinas per group) and calculated and averaged in relation to the endothelial cell area in each individual field. Total endothelial cell area was quantified using Volocity (Improvision).

32. Osoegawa, K. *et al.* Bacterial artificial chromosome libraries for mouse sequencing and functional analysis. *Genome Res.* **10,** 116–128 (2000).
33. Feil, R., Wagner, J., Metzger, D. & Chambon, P. Regulation of Cre recombinase activity by mutated estrogen receptor ligand-binding domains. *Biochem. Biophys. Res. Commun.* **237,** 752–757 (1997).
34. Copeland, N. G., Jenkins, N. A. & Court, D. L. Recombineering: a powerful new tool for mouse functional genomics. *Nature Rev. Genet.* **2,** 769–779 (2001).
35. Soriano, P. Generalized lacZ expression with the ROSA26 Cre reporter strain. *Nature Genet.* **21,** 70–71 (1999).
36. Jat, P. S. *et al.* Direct derivation of conditionally immortal cell lines from an H-2Kb-tsA58 transgenic mouse. *Proc. Natl Acad. Sci. USA* **88,** 5096–5100 (1991).
37. Morgan, S. M., Samulowitz, U., Darley, L., Simmons, D. L. & Vestweber, D. Biochemical characterization and molecular cloning of a novel endothelial-specific sialomucin. *Blood* **93,** 165–175 (1999).
38. Lawson, N. D. & Weinstein, B. M. *In vivo* imaging of embryonic vascular development using transgenic zebrafish. *Dev. Biol.* **248,** 307–318 (2002).